

## Catalysis

## Facile and Flexible Preparation of Highly Active CuCe Monolithic Catalysts for VOCs Combustion

Xiao Chen,<sup>[a]</sup> Qinqi Xu,<sup>[a]</sup> Ying Zhou,<sup>[b]</sup> Qiulian Zhu,<sup>[b]</sup> Haifeng Huang,<sup>[a]</sup> Zhiyan Pan,<sup>[a]</sup> Pengfei Zhang,<sup>[c]</sup> Sheng Dai,<sup>[c]</sup> and Hanfeng Lu<sup>\*[b]</sup>

A novel and practical strategy of preparing mixed oxides/monolithic catalysts for exhaust gas purification is presented in this work. Highly active nano-CuCe catalyst dispersion liquid is synthesized through solvothermal method, and then various CuCe monolithic catalysts are prepared just by a simple spraying method. The as-prepared catalysts showed excellent activity and stability for volatile organic compounds (VOCs) destruction, which can be attributed to the good structural and chemical properties of the well-dispersed CuCe active species on the carrier surface. This strategy provides a very facile and flexible way for preparation of monolithic catalysts with versatile shapes to accommodate VOCs combustion facilities. It shows great potential in practical applications.

Rapid industrialization has greatly improved the human life worldwide but also leads to increased gaseous pollutant emissions and worsened air pollution problems.<sup>[1–4]</sup> The United Nations Environment Program stated that air pollution is one of the world's largest environmental problems that threaten the human health. Thus, air quality must be improved.

Catalytic technology is a unique solution for air pollution control and energy conservation; this technology includes automobile exhaust gas purification, SO<sub>x</sub> and NO<sub>x</sub> removal, VOCs catalytic oxidation, and catalytic combustion, etc.<sup>[5]</sup> Currently, industrial exhaust gas purification mainly uses honeycomb monolithic catalysts.<sup>[6,7]</sup> However, the application of these catalysts is usually limited by their carrier shapes. As such, a large reaction unit must be designed to place the catalyst in the industrial exhaust gas purification system. But if the catalyst

can be placed in the entire purification system (from the inlet to the outlet), then exhaust gas will be purified in any part of the system, resulting in increased catalytic capacity and reduced occupied area of the system. At present, preparation of monolithic catalysts is cumbersome and involves the following steps: the washcoat is coated on the surface of the structured monolithic substrate, followed by loading of the active species through impregnation; or the slurry which is prepared from powder catalyst is directly coated on the surface of the structured monolithic substrate; finally, obtaining the monolithic catalyst through the activation treatment.<sup>[8]</sup> The use of state-of-art methods to load the active species on the entire non-structured exhaust gas purification system is a complex process. However, if the active nanoparticles are in liquid form, then the preparation procedure of the monolithic catalysts can be greatly simplified. Simple spraying can be employed to randomly load the active species in the exhaust gas purification system; in this way, the pipes and refractory bricks can become the exhaust gas purification system. Also the catalyst deactivation is not an issue to be addressed, since it can be reactivated by spraying again, thereby reducing the amount of hazardous wastes generated. As compared with conventional ways to prepare monolithic catalysts, the proposed spraying strategy in current work exhibits the following advantages: (1) The objects of any shape can be modified as monolithic catalysts through simple spraying. This method is more facile and flexible in industrial operation than dipping and coating methods. (2) Once the entire industrial exhaust gas purification device loads the active species, the volume of the reaction chamber can be reduced, in turn the cost and occupied area of facilities are reduced. (3) The catalyst deactivated can be reactivated by spraying again, thereby minimizing hazardous waste generation, and (4) the catalysts can be accommodated to various exhaust gases by spraying the corresponding active dispersion liquid, showing the great potential in practical applications.

Solvothermal method is an effective and simple method currently reported for preparing magnetic monodispersed nanoparticles.<sup>[9–11]</sup> The metal precursors decompose to form nanoparticles in high-boiling solvent, and the resulting metal nanoparticles can be monodispersed in the organic solution thanks to the protection by the surfactant. Hyeon et al.<sup>[12]</sup> synthesized  $\gamma$ -Fe<sub>2</sub>O<sub>3</sub> nanoparticles that can be easily dispersed in hydrocarbon solvents by thermal decomposition of Fe(CO)<sub>5</sub> in a mixture of octyl ether, oleic acid, and dehydrated (CH<sub>3</sub>)<sub>3</sub>NO under argon atmosphere. Sun et al.<sup>[13]</sup> synthesized Fe<sub>3</sub>O<sub>4</sub> nanoparticles that can be easily dispersed in hydrocarbon solvents

[a] X. Chen, Q. Xu, Prof. H. Huang, Prof. Z. Pan  
College of environment  
Zhejiang University of Technology  
Hangzhou 310014, China  
E-mail: hhf66@zjut.edu.cn

[b] Y. Zhou, Q. Zhu, Prof. H. Lu  
College of Chemical Engineering  
Zhejiang University of Technology  
Hangzhou 310014, China  
Tel: +86-571-88320767  
E-mail: luhf@zjut.edu.cn

[c] Prof. P. Zhang, Prof. S. Dai  
Chemical Sciences Division  
Oak Ridge National Laboratory  
Oak Ridge, Tennessee 37831, USA.  
E-mail: dais@ornl.gov

Supporting information for this article is available on the WWW under <https://doi.org/10.1002/slct.201701850>

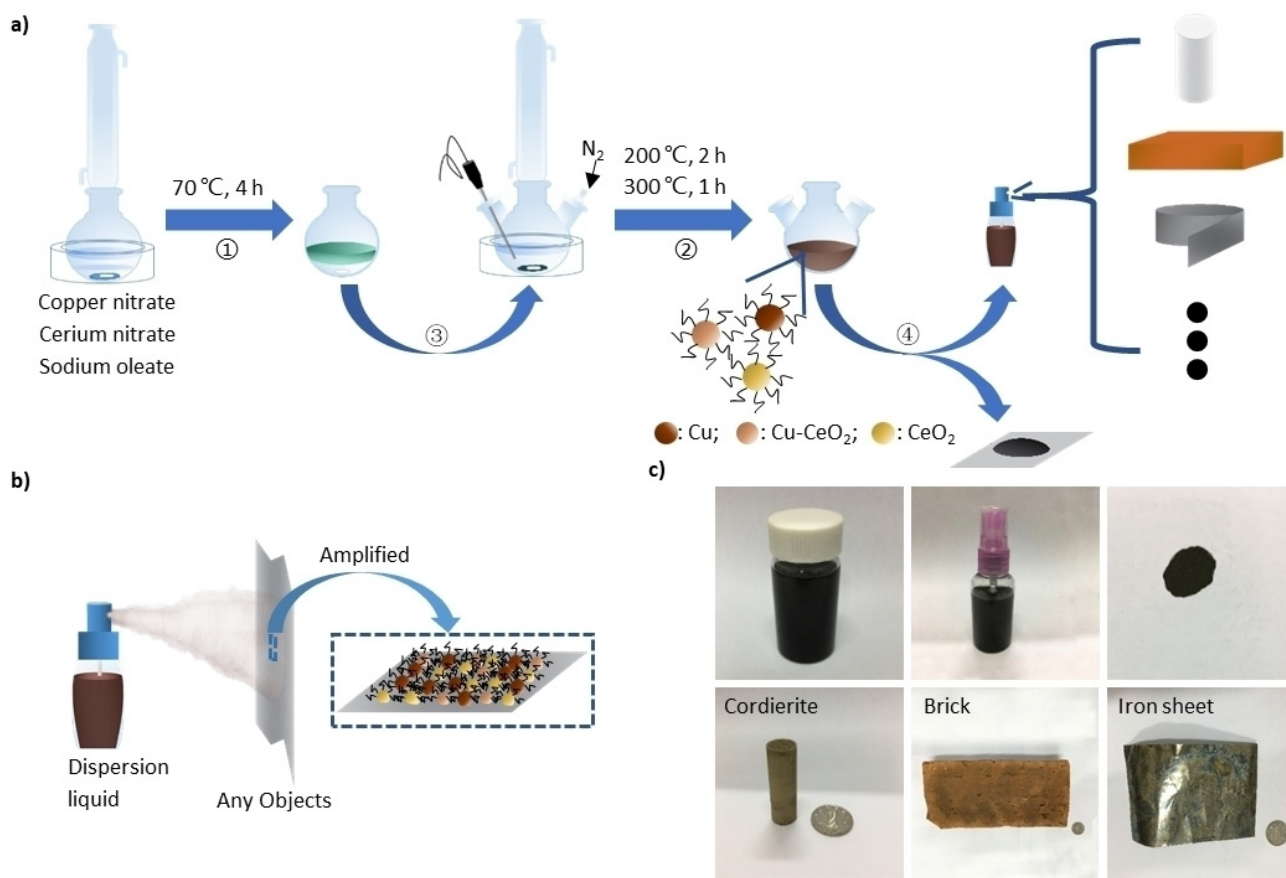


**Figure 1.** (a) The scheme of preparation and application of nano-CuCe dispersion liquid. ① In the mixed solution of n-hexane, ethanol and deionized water, ② In a mixture of oleylamine and oleic acid, ③ Washed with deionized water, and the supernatant solution was evaporated to a three-necked flask, ④ Washed with ethanol and centrifugal separation, then directly calcined to form the powder catalyst or re-dispersed in hexane for storage and sprayed on any object surface to form the supported catalyst; (b) The schematic diagram of loaded CuCe by spray; (c) The photos of dispersion liquid, powder catalyst and the carriers (cordierite, brick, iron sheet) sprayed by nano-CuCe dispersion liquid.

by thermal decomposition of  $\text{Fe}(\text{acac})_3$  in a mixture of phenyl ether, 1,2-hexadecanediol, oleic acid, and oleylamine under nitrogen atmosphere. Park et al.<sup>[14]</sup> synthesized  $\text{Mn}_3\text{O}_4$  nanoparticles that can be easily dispersed in hydrocarbon solvents by thermal decomposition of  $\text{Mn}(\text{acac})_2$  in oleylamine at 180 °C for 9 h under argon atmosphere. However, producing active nano-bimetallic oxide dispersion liquid remains challenging. To the best of our knowledge, there has been few reports.

CuCe bimetallic oxide is an effective oxidation catalyst used in various reactions due to its excellent redox performance and oxygen storage/release capability.<sup>[15–20]</sup> This work aims to introduce a novel and practical strategy of preparing mixed oxides/monolithic catalysts for exhaust gas purification by discussing the preparation of CuCe monolithic catalysts. The prepared catalysts display excellent catalytic activity in the simulation experiment.

The nano-CuCe dispersion liquid is prepared and applied as follows (Figure 1a and see Supporting Information). First, copper and cerium oleate complex was prepared by reacting sodium oleate with  $\text{Ce}(\text{NO}_3)_3 \cdot 6\text{H}_2\text{O}$  and  $\text{Cu}(\text{NO}_3)_2 \cdot 3\text{H}_2\text{O}$  in mixture solvent (ethanol, deionized water, and hexane). After

washing, hexane was removed through evaporation. Then copper and cerium oleate complex and oleic acid were dissolved in oleylamine. The solution was heated to reflux under nitrogen atmosphere and magnetically stirred for a certain time. The cooled solution was then added with ethanol to induce precipitation, and the precipitates were separated from the solvent through centrifugation. The precipitate can be directly calcined to form a powder catalyst, easily re-dispersed in hexane for storage, or sprayed on any object surface to form monolithic catalysts. We selected cordierite honeycomb, brick, and metal sheet to simulate the monolithic catalyst carrier, chimney and piping material in an industrial exhaust gas purification device. These materials were sprayed with the prepared nano-CuCe dispersion liquid (Figure 1b; Supplementary Movie). The photos of dispersion liquid, powder catalyst, and monolithic catalysts are shown in Figure 1c. The dispersion liquid was characterized by TEM and XRD analyses to verify the formation of the active phase in the dispersion liquid (Figures 2a, b, and g). The results show the presence of  $\text{CeO}_2$  and Cu phases, indicating that the dispersion liquid exhibits certain catalytic ability. We sprayed the CuCe dispersion liquid

on cordierite without further treatment, and the activity of the liquid was evaluated by toluene catalytic combustion experiment. The catalyst immediately exhibited high activity when reaching a certain temperature (Figure 3a). Hence, the any object sprayed with the dispersion liquid can be used as catalyst without further treatment.

XRD, TEM, and BET analyses were conducted to investigate the intrinsic structure of CuCe catalyst prepared by solvothermal method. As shown in the TEM image, the particle size was less than 10 nm (Figure 2c). The XRD analysis shows that the

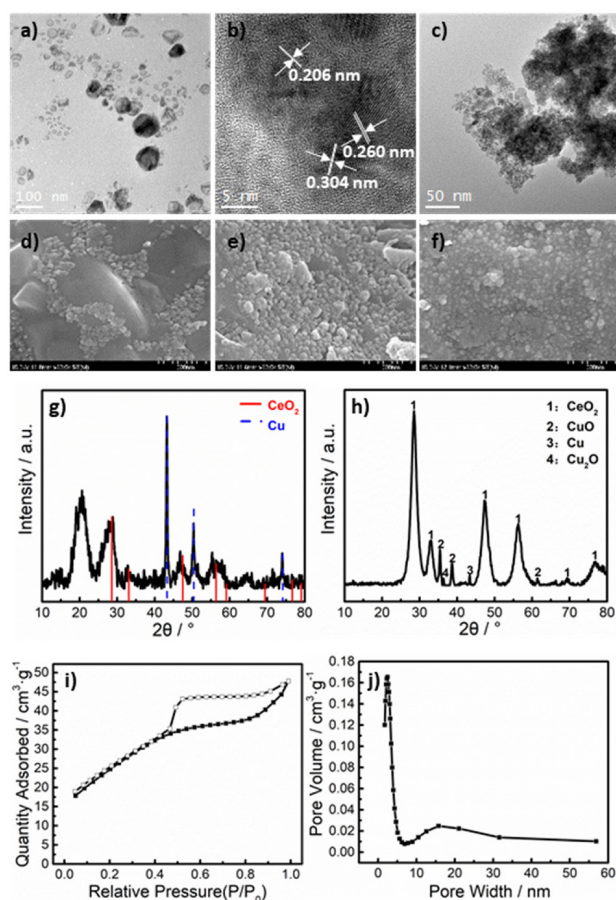


**Figure 2.** (a-b) TEM (100 nm) and HRTEM (5 nm) images of nano-CuCe dispersion liquid; (c) TEM (50 nm) image of CuCe powder catalyst; (d-f) SEM (500 nm) images of the carriers (cordierite, brick, iron sheet) sprayed by nano-CuCe dispersion liquid; (g) XRD pattern of nano-CuCe dispersion liquid; (h) XRD pattern of CuCe powder catalyst; (i) N<sub>2</sub> sorption isotherm of CuCe powder catalyst; (j) BJH adsorption pore-size distributions of CuCe powder catalyst.

major phase was CeO<sub>2</sub> and CuO (Figure 2h). The lattice parameters (5.4051 Å) of the sample were reduced, and the 2θ angle (28.580°) of CeO<sub>2</sub> (111) increased compared with the standard CeO<sub>2</sub> (5.4113 Å, 28.554°). This phenomenon occurred because the Cu ions are partly incorporated into the cerium crystallites. The created oxygen vacancy can improve the catalytic activity. The isotherm curve was a typical IV curve with an obvious H4-type hysteresis loop (Figure 2i).<sup>[21]</sup> The BJH pore

size was 3.4 nm, indicating the formation of the mesopores of the CuCe catalyst (Figure 2j). The surface area of the sample was 90.3 m<sup>2</sup>•g<sup>-1</sup> (Table S1, see Supporting Information), which is larger than that of R-CuCe (26.6 m<sup>2</sup>•g<sup>-1</sup>) prepared by citric acid sol-gel method (see Supporting Information). The catalyst prepared by solvothermal method possesses an improved structure than that prepared by citric acid sol-gel method (Figure S4, Table S1, see Supporting Information).

Raman and H<sub>2</sub>-TPR spectroscopy analyses were conducted to investigate the intrinsic chemical properties of CuCe catalyst prepared by solvothermal method. In the Raman spectra (Figure 3b), the peak at 460 cm<sup>-1</sup> is attributed to the F<sub>2g</sub> Raman

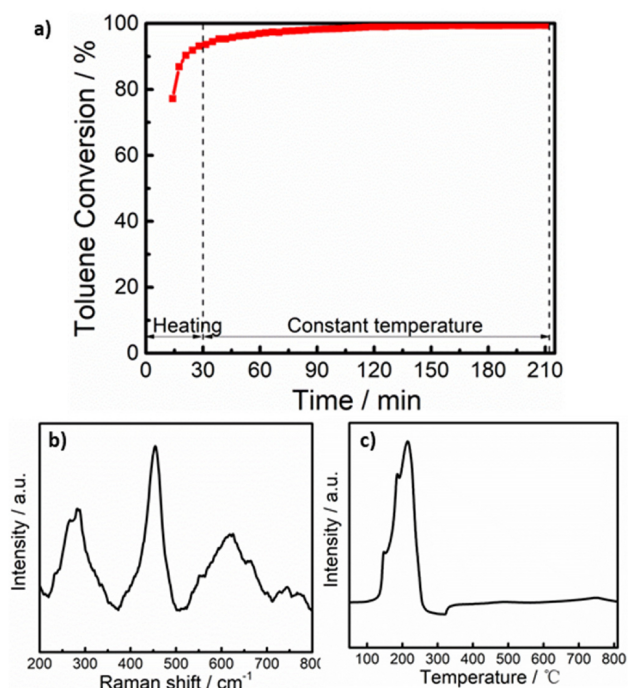


**Figure 3.** (a) Toluene catalytic combustion activity of nano-CuCe dispersion liquid (from room temperature to 300 °C at 10 k/min and maintain 3 h); (b) Raman spectra of CuCe powder catalyst; (c) H<sub>2</sub>-TPR profiles of CuCe powder catalyst.

mode of the symmetric structure of ceria. Meanwhile, a broad peak between about 500 and 700 cm<sup>-1</sup>, which has been related to the presence of oxygen vacancies.<sup>[22-24]</sup> It is a consequence of substitutional incorporation of Cu<sup>2+</sup> into the ceria lattice, which could be accompanied by the generation of oxygen vacancies according to the charge balance. As previously reported,<sup>[22]</sup> the larger area ratio of about 610 cm<sup>-1</sup> to 460 cm<sup>-1</sup>, the more the relative concentration of oxygen vacancies. The data (1.1:0.7) imply that CuCe catalyst prepared by solvothermal method contain more oxygen vacancies than that prepared by citric acid sol-gel method (Figure S5a, Table S2, see Supporting Information). The redox properties of the CuCe catalysts were evaluated by H<sub>2</sub>-TPR analysis. Pure CuO was characterized by a single reduction peak at above 300 °C. In the H<sub>2</sub>-TPR curve (Figure 3c), the reduction peak of CuCe was

reduced to 215 °C, which is lower than that of R-CuCe (Figure S5b, see Supporting Information), and the total H<sub>2</sub> consumption levels of CuCe are higher (Table S2, see Supporting Information). Solvothermal method significantly improved the oxygen activity of the CuCe catalyst. This improved activity is highly beneficial for heterogeneous catalytic oxidation reactions.<sup>[25]</sup> The catalytic performance of the fabricated CuCe catalyst was evaluated for catalytic combustion of VOCs, such as toluene, hexane, and ethanol. The results show that CuCe catalyst prepared by solvothermal method exhibits excellent catalytic activity (Figures 4a, S6, see Supporting Information).

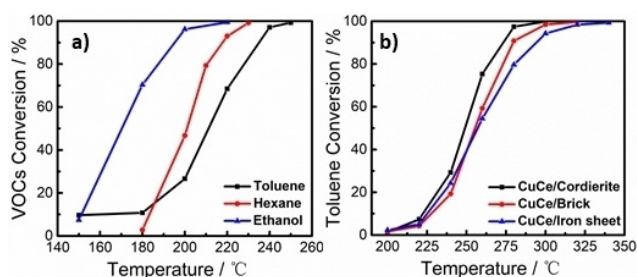


**Figure 4.** (a) Light-off curves of VOCs (toluene, hexane and ethanol) catalytic combustion on CuCe powder catalysts; (b) Light-off curves of toluene catalytic combustion on monolithic catalysts (cordierite, brick, iron sheet).

This finding provides strong support for subsequent spray application of nano-CuCe dispersion liquid.

To simulate the various parts of the catalyst-loaded industrial exhaust gas purification device, we sprayed the nano-CuCe dispersion liquid onto the cordierite, brick, and iron sheet to form the monolithic catalysts. As shown in the SEM images (Figures 2d, e, and f), the active species are well-dispersed on the surface of each carrier, which is highly beneficial for heterogeneous catalytic oxidation reactions. We investigated the catalytic effect at different temperatures. In the toluene catalytic combustion experiments (Figures 4b, S8, see Supporting Information), the monolithic catalysts prepared by spraying the nano-CuCe dispersion liquid exhibit improved catalytic activity. The toluene conversion rate reached 95% or more at 300 °C under the experimental conditions. As such, the proposed method exhibits potential for practical application. In addition, the experimental results of the catalytic combustion of hexane and ethanol confirmed the advantages of this strategy (Figures S9 and S10, see Supporting Information).

Here we propose a novel and practical strategy for preparing mixed oxides/monolithic catalysts for exhaust gas purification. First, the highly active nano-CuCe dispersion liquid is synthesized, and then CuCe monolithic catalysts are produced by simply spraying on any object. This strategy makes preparation of monolithic catalysts become facile and flexible. Meanwhile, these CuCe monolithic catalysts exhibit extremely high activity and stability (Figure S11, see Supporting Information) in the catalytic combustion of VOCs. It can be attributed to the CuCe active species with good structure and chemical properties are well-dispersed on the carrier surface. The other

bimetallic oxide catalysts prepared using this method also showed excellent activity in the toluene catalytic combustion experiments (Figure S12, see Supporting Information). This strategy exhibits great potential in practical application and will be an interesting research domain. Dispersion liquids can be prepared depending on the type of exhaust gas. These liquids like automobile exhaust gas purification catalyst and formaldehyde oxidation catalyst, which can be sprayed on the vehicle exhaust pipe or the objects in the room to induce their catalytic activity. Although just upon simply spraying, the active species can be well-dispersed on the carrier surface. We believe that this strategy will provide new ideas of preparation monolithic catalysts and additional insights into general catalyst design.

## Supporting Information Summary

The details of catalyst preparation, characterization and activity test are included in the experimental. Additional figures and tables display the more results for characterization and reaction of catalysts.

## Acknowledgements

This work was supported by the Natural Science Foundation of China (No. 21506194, 21676255) and the Natural Science Foundation of Zhejiang Province (No. Y16B070011). The Commission of Science and Technology of Zhejiang province (No. 2017C03007, 2017C33106).

## Conflict of Interest

The authors declare no conflict of interest.

**Keywords:** dispersion liquid · heterogeneous catalysis · monolithic catalysts · nanoparticles · VOCs

- [1] X. T. Zeng, Y. F. Tong, L. Cui, X. M. Kong, Y. N. Sheng, L. Chen, Y. P. Li, *J. Environ. Manage.* **2017**, *197*, 507–521.
- [2] D. Tilman, K. G. Cassman, P. A. Matson, R. Naylor, S. Polasky, *Nature* **2002**, *418*, 671–677.
- [3] X. T. Zeng, G. H. Huang, H. L. Chen, Y. P. Li, X. M. Kong, Y. R. Fan, *Ecol. Modell.* **2016**, *334*, 60–77.
- [4] B. A. Kathleen, R. T. Raymond, B. C. Alvin, B. C. Jose, *J. Cleaner Prod.* **2011**, *19*, 187–196.
- [5] H. X. Dai, *Sci. Bull.* **2015**, *60*, 1708–1710.
- [6] D. M. Gomez, J. M. Gatica, J. C. Hernandez-Garrido, G. A. Cifredo, M. Montes, O. Sanz, J. M. Rebled, H. Vidal, *Appl. Catal., B* **2014**, *144*, 425–434.
- [7] A. Cybulski, J. A. Moulijn, *Catal. Rev.: Sci. Eng.* **2006**, *36*, 179–270.
- [8] P. Avila, M. Montes, E. E. Miro, *Chem. Eng. J.* **2005**, *109*, 11–36.
- [9] S. Laurent, D. Forge, M. Port, A. Roch, C. Robic, L. V. Elst, R. N. Muller, *Chem. Rev.* **2008**, *108*, 2064–2110.
- [10] A. H. Lu, E. L. Salabas, F. Schuth, *Angew. Chem., Int. Ed.* **2007**, *46*, 1222–1244.
- [11] L. H. Wu, A. Mendoza-Garcia, L. Qing, S. H. Sun, *Chem. Rev.* **2016**, *116*, 10473–10512.
- [12] T. Hyeon, S. L. Su, J. Park, Y. Chung, H. B. Na, *J. Am. Chem. Soc.* **2001**, *123*, 12798–12801.
- [13] S. H. Sun, H. Zeng, *J. Am. Chem. Soc.* **2002**, *124*, 8204–8205.

- [14] W. S. Seo, H. H. Jo, K. Lee, B. Kim, S. J. Oh, J. T. Park, *Angew. Chem., Int. Ed.* **2004**, *43*, 1115–1117.
- [15] C. L. Zhu, T. Ding, W. X. Gao, B. Kim, K. Ma, Y. Tian, X. A. Li, *Int. J. Hydrogen Energy* **2017**, *42*, 17457–17465.
- [16] D. Delimaris, T. Ioannides, *Appl. Catal., B* **2009**, *89*, 295–302.
- [17] T. Tsoncheva, G. Issa, T. Blasco, M. Dimitrov, M. Popova, S. Hernandez, D. Kovacheva, G. Atanasova, J. M. L. Nieto, *Appl. Catal., A* **2013**, *453*, 1–12.
- [18] J. J. Sheng, C. Li, L. K. Zhao, X. Y. Du, L. Gao, G. M. Zeng, *Fuel* **2017**, *197*, 397–406.
- [19] R. Dziembaj, M. Molenda, L. Chmielarz, M. M. Zaitz, Z. Piwowarka, A. Rafalska-Lasocha, *Catal. Today* **2011**, *169*, 112–117.
- [20] X. B. Zhu, X. Gao, R. Qin, Y. X. Zeng, R. Y. Qu, C. H. Zheng, X. Tu, *Appl. Catal., B* **2015**, *170–171*, 293–300.
- [21] Y. H. Cao, K. L. Wang, X. M. Wang, Z. R. Gu, Q. H. Fan, W. Gibbons, J. D. Hoefelmeyer, P. R. Kharel, M. Shrestha, *Electrochim. Acta* **2016**, *212*, 839–847.
- [22] Y. J. Luo, K. C. Wang, Y. X. Xu, X. Y. Wang, Q. R. Qian, Q. H. Chen, *New J. Chem.* **2015**, *39*, 1001–1005.
- [23] J. R. McBride, K. C. Hass, B. D. Poindexter, W. H. Weber, *J. Appl. Phys.* **1994**, *76*, 2345–2441.
- [24] X. Q. Wang, J. A. Rodriguez, J. C. Hanson, D. Gamarra, A. Martínez-Arias, M. Fernández-García, *J. Phys. Chem. B* **2005**, *109*, 19595–19603.
- [25] H. F. Lu, P. F. Zhang, Z. A. Qiao, J. S. Zhang, H. Y. Zhu, J. H. Chen, Y. F. Chen, S. Dai, *Chem. Commun.* **2015**, *51*, 5910–5913

Submitted: August 14, 2017

Revised: September 24, 2017

Accepted: September 26, 2017